
Compact Deep Aggregation for Set Retrieval

Yujie Zhong · Relja Arandjelović · Andrew Zisserman

Abstract The objective of this work is to learn a compact embedding of a set of descriptors that is suitable for efficient retrieval and ranking, whilst maintaining discriminability of the individual descriptors. We focus on a specific example of this general problem – that of retrieving images containing multiple faces from a large scale dataset of images. Here the set consists of the face descriptors in each image, and given a query for multiple identities, the goal is then to retrieve, in order, images which contain all the identities, all but one, etc.

To this end, we make the following contributions: first, we propose a CNN architecture – *SetNet* – to achieve the objective: it learns face descriptors and their aggregation over a set to produce a compact fixed length descriptor designed for set retrieval, and the score of an image is a count of the number of identities that match the query; second, we show that this compact descriptor has minimal loss of discriminability up to two faces per image, and degrades slowly after that – far exceeding a number of baselines; third, we explore the speed vs. retrieval quality trade-off for set retrieval using this compact descriptor; and, finally, we collect and annotate a large dataset of images containing various number of celebrities, which we use for evaluation and is publicly released.

Keywords Image retrieval · Set retrieval · Face recognition · Descriptor aggregation · Representation learning · Deep learning

1 Introduction

Suppose we wish to retrieve all images in a very large collection of personal photos that contain a particular set of people,

Y. Zhong and A. Zisserman
Visual Geometry Group, Department of Engineering Science, University of Oxford, UK
E-mail: {yujie,az}@robots.ox.ac.uk

R. Arandjelović
DeepMind
E-mail: relja@google.com

such as a group of friends or a family. Then we would like the retrieved images that contain all of the set to be ranked first, followed by images containing subsets, e.g. if there are three friends in the query, then first would be images containing all three friends, then images containing two of the three, followed by images containing only one of them. Consider another example where a fashion savvy customer is researching a dress and a handbag. A useful retrieval system would first retrieve images in which models or celebrities wear both items, so that the customer can see if they match. Following these, it would also be beneficial to show images containing any one of the query items so that the customer can discover other fashionable combinations relevant to their interest. For these systems to be of practical use, we would also like this retrieval to happen in real time.

These are examples of a *set retrieval problem*: the database consists of many sets of elements (e.g. the set is an image containing multiple faces, or of a person with multiple fashion items), and we wish to order the sets according to a query (e.g. multiple identities, or multiple fashion items) such that those sets satisfying the query completely are ranked first (i.e. those images that contain all the identities of the query, or all the query fashion items), followed by sets that satisfy all but one of the query elements, etc. An example of this ranking for the face retrieval problem is shown in Fig. 1 for two queries.

In this work, we focus on the problem of retrieving a set of identities, but the same approach can be used for other set retrieval problems such as the aforementioned fashion retrieval. We can operationalize this by scoring each face in each photo of the collection as to whether they are one of the identities in the query. Each face is represented by a fixed length vector, and identities are scored by logistic regression classifiers. But, consider the situation where the dataset is very large, containing millions or billions of images each containing multiple faces. In this situation two aspects are crucial for real time retrieval: first, that all operations take place in memory (not reading from disk), and second that an

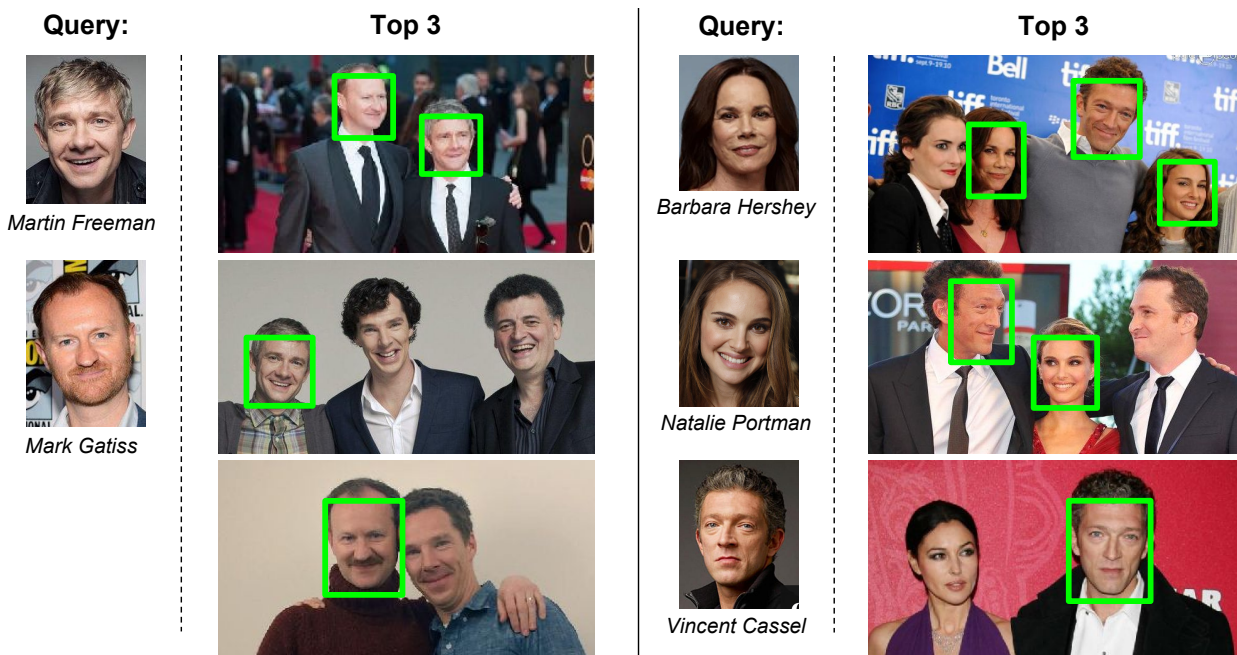


Fig. 1: **Images ranked using set retrieval for two example queries.** The query faces are given on the left of each example column, together with their names (only for reference). Left: a query for two identities; right: a query for three identities. The first ranked image in each case contains all the faces in the query. Lower ranked images partially satisfy the query, and contain progressively fewer faces of the query. The results are obtained using the compact set retrieval descriptor generated by the SetNet architecture, by searching over 200k images of the *Celebrity Together* dataset introduced in this paper.

efficient algorithm is used when searching for images that satisfy the query. The problem is that storing a fixed length vector for each *face* in memory is prohibitively expensive at this scale, but this cost can be significantly reduced if a fixed length vector is only stored for each *set of faces* in an image (since there are far fewer images than faces). As well as reducing the memory cost this also reduces the run time cost of the search since fewer vectors need to be scored.

So, the question we investigate in this paper is the following: can we aggregate the *set of vectors* representing the multiple faces in an image into a *single vector* with little loss of set-retrieval performance? If so, then the cost of both memory and retrieval can be significantly reduced as only one vector per *image* (rather than one per *face*) have to be stored and scored.

Although we have motivated this question by face retrieval it is quite general: there is a set of elements (which are permutation-invariant), each element is represented by a vector of dimension D_e , and we wish to represent this set by a single vector of dimension D , where $D = D_e$ in practice, without losing information essential for the task. Of course, if the total number of elements in all sets, N , is such that $N \leq D$ then this certainly can be achieved provided that the set of vectors are orthogonal. However, we will consider the situation commonly found in practice where $N \gg D$, e.g. D

is small, typically 128 (to keep the memory footprint low), and N is in the thousands.

We make the following contributions: first, we introduce a trainable CNN architecture for the set-retrieval task that is able to learn to aggregate face vectors into a fixed length descriptor in order to minimize interference, and also is able to rank the face sets according to how many identities are in common with the query using this descriptor. To do this, we propose a paradigm shift where we draw motivation from image retrieval based on local descriptors. In image retrieval, it is common practice to aggregate all local descriptors of an image into a fixed-size image-level vector representation, such as bag-of-words (Sivic and Zisserman, 2003) and VLAD (Jégou et al., 2010); this brings both memory and speed improvements over storing all local descriptors individually. We generalize this concept to set retrieval, where instead of aggregating local interest point descriptors, set element descriptors are pooled into a single fixed-size set-level representation. For the particular case of face set retrieval, this corresponds to aggregating face descriptors into a set representation. The novel aggregation procedure is described in Sec. 3 where the aggregator can be trained in an end-to-end manner with different feature extractor CNNs.

Our second contribution is to introduce a dataset annotated with multiple faces per images. In Sec. 4 we describe

a pipeline for automatically generating a labelled dataset of pairs (or more) of celebrities per image. This *Celebrity Together* dataset contains around 200k images with more than half a million faces in total. It is publicly released.

The performance of the set-level descriptors is evaluated in Sec. 5. We first ‘stress test’ the descriptors by progressively increasing the number of faces in each set, and monitoring their retrieval performance. We also evaluate retrieval on the *Celebrity Together* dataset, where images contain a variable number of faces, with many not corresponding to the queries, and explore efficient algorithms that can achieve immediate (real-time) retrieval on very large scale datasets. Finally, we investigate what the trained network learns by analyzing why the face descriptors learnt by the network are well suited for aggregation.

Note, although we have grounded the set retrieval problem as faces, the treatment is quite general: it only assumes that dataset elements are represented by vectors and the scoring function is a scalar product. We return to this point in the conclusion.

2 Related work

To the best of our knowledge, this paper is the first to consider the set retrieval problem. However, the general area of image retrieval has an extensive literature that we build on here.

2.1 Aggregating descriptors

One of the central problems that has been studied in large scale image instance retrieval is how to condense the information stored in multiple local descriptors such as SIFT (Lowe, 2004), into a single compact vector to represent the image. This problem has been driven by the need to keep the memory footprint low for very large image datasets. An early approach is to cluster descriptors into visual words and represent the image as a histogram of word occurrences – bag-of-visual-words (Sivic and Zisserman, 2003). Performance can be improved by aggregating local descriptors within each cluster, in representations such as Fisher Vectors (Jégou et al., 2011; Perronnin et al., 2010a) and VLAD (Jégou et al., 2010). In particular, VLAD – ‘Vector of Locally Aggregated Descriptors’ by Jégou et al. (2010) and its improvements (Arandjelović and Zisserman, 2013; Delhumeau et al., 2013; Jégou and Zisserman, 2014) was used to obtain very compact descriptions via dimensionality reduction by PCA, considerably reducing the memory requirements compared to earlier bag-of-words based methods (Chum et al., 2007; Nister and Stewenius, 2006; Philbin et al., 2007; Sivic and Zisserman, 2003). VLAD has superior ability in maintaining the information about individual local descriptors while performing aggressive dimensionality reduction.

VLAD has recently been adapted into a differentiable CNN layer, NetVLAD (Arandjelović et al., 2016), making it end-to-end trainable. We incorporate a modified form of the NetVLAD layer in our SetNet architecture. An alternative, but related, very recent approach is the memory vector formulation proposed by Iscen et al. (2017), but we have not employed it here as it has not been made differentiable yet.

2.2 Image retrieval

Another strand of research we build on is category level retrieval, where in our case the category is a face. This is another classical area of interest with many related works (Chatfield et al., 2011; Perronnin et al., 2010b; Torresani et al., 2010; Wang et al., 2010; Zhou et al., 2010). Since the advent of deep CNNs (Krizhevsky et al., 2012), the standard solution has been to use features from the last hidden layer of a CNN trained on ImageNet (Donahue et al., 2013; Razavian et al., 2014; Sermanet et al., 2013) as the image representation. This has enabled a very successful approach for retrieving images containing the query category by training linear SVMs on-the-fly and ranking images based on their classification scores (Chatfield et al., 2014, 2015). For the case of faces, the feature vector is produced from the face region using a CNN trained to classify or embed faces (Parkhi et al., 2015; Schroff et al., 2015; Taigman et al., 2014). Li et al. (2011) tackle face retrieval by using binary codes that jointly encode identity discriminability and a number of facial attributes. Li et al. (2015) extend image-based face retrieval to video scenarios, and learn low-dimensional binary vectors encoding the face tracks and hierarchical video representations.

Apart from single-object retrieval, there are also works on compound query retrieval, such as (Zhong et al., 2016) who focus on finding a specific face in a place. While this can be seen as set retrieval where each set has exactly two elements, one face and one place, it is not applicable to our problem as their elements come from different sources (two different networks) and are never combined together in a set-level representation.

2.3 Approaches for sets

Also relevant are works that explicitly deal with sets of vectors. Kondor and Jebara (2003) developed a kernel between vector sets by characterising each set as a Gaussian in some Hilbert space. However, their set representation cannot currently be combined with CNNs and trained in an end-to-end fashion. Feng et al. (2017) learn a compact set representation for matching of image sets by jointly optimizing a neural network and hashing functions in an end-to-end fashion. Pooling architectures are commonly used to deal with sets, e.g. for combining information from a set of views for 3D shape

recognition (Shi et al., 2015; Su et al., 2015). Zaheer et al. (2017) investigate permutation-invariant objective functions for operating on sets, although their method boils down to average pooling of input vectors, which we compare to as a baseline. Some works adopt attention mechanism (Ilse et al., 2018; Lee et al., 2018; Vinyals et al., 2016; Yang et al., 2018) or relational network (Santoro et al., 2017) into set operations to model the interactions between elements in the input set. Hamid Rezaatofghi et al. (2017) consider the problem of predicting sets, i.e. having a network which outputs sets, rather than our case where a set of elements is an input to be processed and described with a single vector. Siddiquie et al. (2011) formulate a face retrieval task where the query is a set of attributes. Yang et al. (2017) and Liu et al. (2017) learn to aggregate set of faces of the same identity for recognition, with different weightings based on image quality using an attention mechanism. For the same task, Wang et al. (2017) represent face image sets as covariance matrices. Note, our objective differs from these: we are not aggregating sets of faces of the same identity, but instead aggregating sets of faces of different identities.

3 SetNet – a CNN for set retrieval

As described in the previous section, using a single fixed-size vector to represent a set of vectors is a highly appealing approach due to its superior speed and memory footprint over storing a descriptor-per-element. In this section, we propose a CNN architecture, *SetNet*, for the end-task of set retrieval. There are two objectives:

1. It should learn the element descriptors together with the aggregation in order to minimise the loss in face classification performance between using individual descriptors for each face, and an aggregated descriptor for the set of faces. This is achieved by training the network for this task, using an architecture combining ResNet for the individual descriptors together with NetVLAD for the aggregation.
2. It should be able to rank the images using the aggregated descriptor in order of the number of faces in each image that correspond to the identities in the query. This is achieved by scoring each face using a logistic regression classifier. Since the score of each classifier lies between 0 and 1, the score for the image can simply be computed as the sum of the individual scores, and this summed score determines the ranking function.

As an example of the scoring function, if the search is for two identities and an image contains faces of both of them (and maybe other faces as well), then the ideal score for each relevant face would be one, and the sum of scores for the image would be two. If an image only contains one of the identities, then the sum of the scores would be one. The images with higher summed scores are then ranked higher

and this naturally orders the images by the number of faces it contains that satisfy the query.

Network Deployment. To deploy the set level descriptor for retrieval in a large scale dataset, there are two stages:

Offline: SetNet is used to compute face descriptors for each face in an image, and aggregate them to generate a set-vector representing the image. This procedure is carried out for every image in the dataset, so that each image is represented by a single vector.

At **run-time**, to search for an identity, a face descriptor is computed for the query face using SetNet, and a logistic regression classifier used to score each image based on the scalar product between its set-vector and the query face descriptor. Searching with a set of identities amounts to summing up the image scores of each query identity.

3.1 SetNet architecture

In this section we introduce our CNN architecture, designed to aggregate multiple element (face) descriptors into a single fixed-size set representation. The *SetNet* architecture (Fig. 2) conceptually has two parts: (i) each face is passed through a feature extractor network separately, producing one descriptor per face; (ii) the multiple face descriptors are aggregated into a single compact vector using a modified NetVLAD layer, followed by a trained dimensionality reduction. At training time, we add a third part which emulates the run-time use of logistic regression classifiers. All three parts of the architecture are described in more detail next.

Feature extraction. The first part is a CNN for feature extraction which produces individual element descriptors (x_1 to x_F), where F is the number of faces in an image. We experiment with two different base architectures – modified ResNet-50 (He et al., 2016) and modified SENet-50 (Hu et al., 2018), both chopped after the global average pooling layer. The ResNet-50 and SENet-50 are modified to produce D_e dimensional vectors (where D_e is 128 or 256) in order to keep the dimensionality of our feature vectors relatively low, and we have not observed a significant drop in face recognition performance from the original 2048-D descriptors. The modification is implemented by adding a fully-connected (FC) layer of size $2048 \times D_e$ after the global average pooling layer of the original network, in order to obtain a lower D_e -dimensional face descriptor. This additional fully-connected layer essentially acts as a dimensionality reduction layer. This modification introduces around 260k additional weights to the network for $D_e = 128$, and 520k weights for $D_e = 256$, which is negligible compared to the total number of parameters of the base networks (25M for ResNet-50, 28M for SENet-50).

Feature aggregation. Face features are aggregated into a single vector V using a NetVLAD layer (illustrated in Fig. 3,

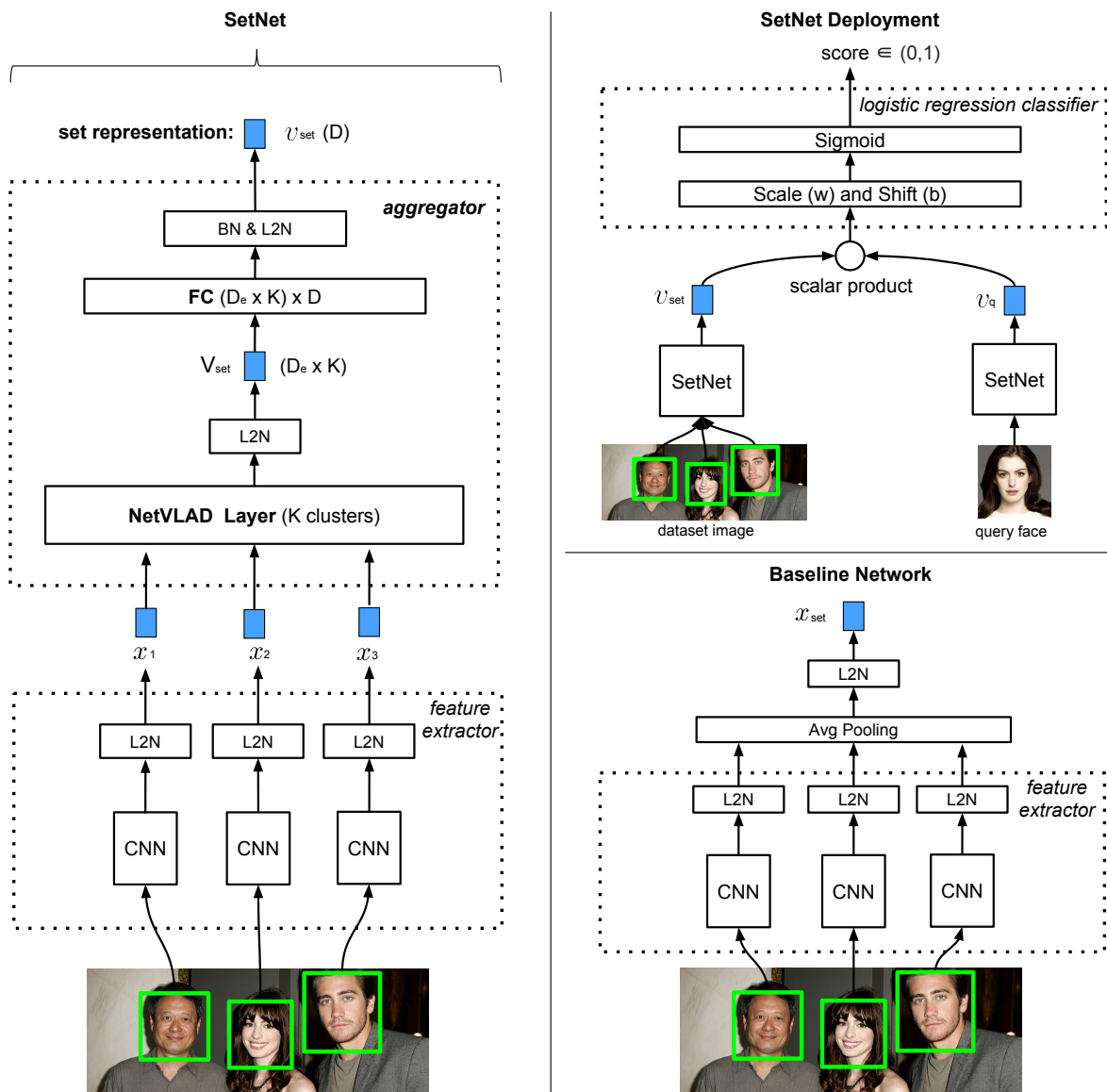


Fig. 2: **SetNet architecture and training.** **Left:** SetNet – features are extracted from each face in an image using a modified ResNet-50 or SENet-50. They are aggregated using a modified NetVLAD layer into a single $D_e \times K$ dimensional vector which is then reduced to D dimension (where D is 128 or 256) via a fully connected dimensionality reduction layer, and L2-normalized to obtain the final image-level compact representation. **Right (top):** at test time, a query descriptor, v_q , is obtained for each query face using SetNet (the face is considered as a single-element set), and the dataset image is scored by a logistic regression classifier on the scalar product between the query descriptor v_q and image set descriptor v_{set} . The final score of an image is then obtained by summing the scores of all the query identities. **Right (bottom):** the baseline network has the same feature extractor as SetNet, but the feature aggregator uses an average-pooling layer, rather than NetVLAD.

and described below in Sec. 3.2). The NetVLAD layer is slightly modified by adding an additional L2-normalization step – the total contribution of each face descriptor to the aggregated sum (i.e. its weighted residuals) is L2-normalized in order for each face descriptor to contribute equally to the final vector; this procedure is an adaptation of residual normalization (Delhumeau et al., 2013) of the vanilla VLAD

to NetVLAD. The NetVLAD-pooled features are reduced to be D -dimensional by means of a fully-connected layer followed by batch-normalization (Ioffe and Szegedy, 2015), and L2-normalized to produce the final set representation v_{set} .

Training block. At training time, an additional logistic regression loss layer is added to mimic the run-time scenario

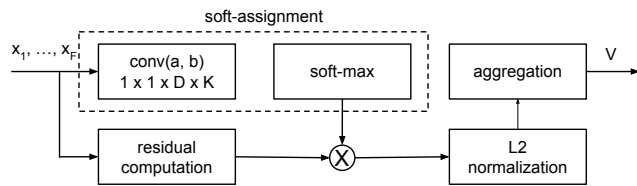


Fig. 3: **NetVLAD layer.** Illustration of the NetVLAD layer (Arandjelović et al., 2016), corresponding to equation (1), and slightly modified to perform L2-normalization before aggregation; see Sec. 3.2 for details.

where a logistic regression classifier is used to score each image based on the scalar product between its set-vector and the query face descriptor. Note, SetNet is used to generate both the set-vector and the face descriptor. Sec. 3.3 describes the appropriate loss and training procedure in more detail.

3.2 NetVLAD trainable pooling

NetVLAD has been shown to outperform sum and max pooling for the same vector dimensionality, which makes it perfectly suited for our task. Here we provide a brief overview of NetVLAD, for full details please refer to (Arandjelović et al., 2016).

For F D -dimensional input descriptors $\{x_i\}$ and a chosen number of clusters K , NetVLAD pooling produces a single $D \times K$ vector V (for convenience written as a $D \times K$ matrix) according to the following equation:

$$V(j, k) = \sum_{i=1}^F \frac{e^{a_k^T x_i + b_k}}{\sum_{k'} e^{a_{k'}^T x_i + b_{k'}}} (x_i(j) - c_k(j)), \quad j \in 1, \dots, D \quad (1)$$

where $\{a_k\}$, $\{b_k\}$ and $\{c_k\}$ are trainable parameters for $k \in [1, 2, \dots, K]$. The first term corresponds to the soft-assignment weight of the input vector x_i for cluster k , while the second term computes the residual between the vector and the cluster centre. Finally, the vector is L2-normalized.

3.3 Loss function and training procedure

In order to achieve the two objectives outlined at the beginning of Sec. 3, a Multi-label logistic regression loss is used. Suppose a particular training image contains F faces, and the mini-batch consists of faces for P identities. Then in a forward pass at training time, the descriptors for the F faces are aggregated into a single feature vector, v_{set} , using the SetNet architecture, and a face descriptor, v_f , is computed using SetNet for each of the faces of the P identities. The training image is then scored for each face f by applying a logistic regressor classifier to the scalar product $v_{set}^T v_f$, and the score should ideally be one for each of the F identities

in the image, and zero for the other $P - F$ faces. The loss measures the deviation from this ideal score, and the network learns to achieve this by maintaining the discriminability for individual face descriptors after aggregation.

In detail, incorporating the loss is achieved by adding an additional layer at training time which contains a logistic regression loss for each of the P training identities, and is trained together with the rest of the network.

Multi-label logistic regression loss. For each training image (set of faces), the loss L is computed as:

$$L = - \sum_{f=1}^P y_f \log(\sigma(w(v_f^T v_{set}) + b)) + (1 - y_f) \log(1 - \sigma(w(v_f^T v_{set}) + b)) \quad (2)$$

where $\sigma(s) = 1/(1 + \exp(-s))$ is a logistic function, P is the number of face descriptors (the size of the mini-batches at training), and w and b are the scaling factor and shifting bias respectively of the logistic regression classifier, and y_f is a binary indicator whether face f is in the image or not. Note that multiple y_f 's are equal to 1 if there are multiple faces which correspond to the identities in the image.

3.4 Implementation details

This section gives full details of the training procedure, including how the network is used at run-time to rank the dataset images given query examples.

Training data. The network is trained using faces from the training partition of the VGGFace2 dataset (Cao et al., 2018). This consists of 8631 identities, with on average 360 face samples for each identity.

Balancing positives and negatives. For each training image (face set) there are many more negatives (the $P - F$ identities outside of the image set) than positives (identities in the set), i.e. most y_f 's in eq. (2) are equal to 0 with only a few 1's. To restore balance, the contributions of the positives and negatives to the loss function is down-weighted by their respective counts.

Initialization and pre-training. A good (and necessary) initialization for the network is obtained as follows. The face feature extraction block is pretrained for single face classification on the VGGFace2 Dataset (Cao et al., 2018) using softmax loss. The NetVLAD layer, with $K = 8$ clusters, is initialized using k-means as in (Arandjelović et al., 2016). The fully-connected layer, used to reduce the NetVLAD dimensionality to D , is initialized by PCA, i.e. by arranging the first D principal components into the weight matrix. Finally, the entire SetNet is trained for face aggregation using the Multi-label logistic regression loss (Sec. 3.3).

Training details. Training requires face set descriptors computed for each image, and query faces (which may or may not occur in the image). The network is trained on synthetic face sets which are built by randomly sampling identities (e.g. two identities per image). For each identity in a synthetic set, two faces are randomly sampled (from the average of 360 for each identity): one contributes to the set descriptor (by combining it with samples of the other identities), the other is used as a query face, and its scalar product is computed with all the set descriptors in the same mini-batch. In our experiments, each mini-batch contains 84 faces. Stochastic gradient descent is used to train the network (implemented in MatConvNet (Vedaldi and Lenc, 2015), with weight decay 0.001, momentum 0.9, and an initial learning rate of 0.001 for pre-training and 0.0001 for fine-tuning; the learning rates are divided by 10 in later epochs).

Faces are detected from images using MTCNN (Zhang et al., 2016). Training faces are resized such that the smallest dimension is 256 and random 224×224 crops are used as inputs to the network. To further augment the training faces, random horizontal flipping and up to 10 degree rotation is performed. At test time, faces are resized so that the smallest dimension is 224 and the central crop is taken.

Dataset retrieval. Suppose we wish to retrieve images containing multiple identities (or a subset of these). First, a face descriptor is produced by *SetNet* for each query face. The face descriptors are then used to score a dataset image for each query identity, followed by summing the individual logistic regression scores to produce the final image score. A ranked list is obtained by sorting the dataset images in non-increasing score order. In the case where multiple face examples are available for a query identity, *SetNet* is used to extract face descriptors and aggregate them to form a richer descriptor for that query identity.

4 ‘Celebrity Together’ dataset

A new dataset, *Celebrity Together*, is collected and annotated. It contains images that portray multiple celebrities simultaneously (Fig. 4 shows a sample), making it ideal for testing set retrieval methods. Unlike the other face datasets, which exclusively contain individual face crops, *Celebrity Together* is made of full images with multiple labelled faces. It contains 194k images and 546k faces in total, averaging 2.8 faces per image. The image collection and annotation procedures are explained next.

4.1 Image collection and annotation procedure

The dataset is created with the aim of containing multiple people per image, which makes the image collection procedure

much more complex than when building a single-face-per-image dataset, such as (Parkhi et al., 2015). The straightforward strategy of (Parkhi et al., 2015), which involves simply searching for celebrities on an online image search engine, is inappropriate: consider an example of searching for Natalie Portman on Google Image Search – *all* top ranked images contain only her and no other person. Here we explain how to overcome this barrier to collect images with multiple celebrities in them.

Query selection. In order to acquire celebrity name pairs, we first perform a search by using ‘seed-celebrity and’, and then scan the meta information for other celebrity names to produce a list of (seed-celebrity, celebrity-friend) pairs. However, one important procedure which is not included in the main paper is that some celebrity may have a strong connection to one or more particular celebrities, which could prevent us from obtaining a diverse list of celebrity friends. For instance, almost all the top 100 images returned by ‘Beyoncé and’ are with her husband Jay Z. Therefore, to prevent such celebrity friends dominating the top returned results, a secondary search is conducted by explicitly removing pairs found by the first-round search, i.e. the query term now is ‘seed-celebrity and -friend1 -friend2 ...’, where *friend1*, *friend2* .. are those found in the first search. We do not perform more searches after the second round, as we find that the number of new pairs obtained in the third-round search is minimal.

Image download and filtering. Once the name pairs are obtained, we download the images and meta information from the image search engine, followed by name scanning again to remove false images. Face detection is performed afterwards to further refine the dataset by removing images with fewer than two faces.

De-duplication. Removal of near duplicate images is performed similarly to (Parkhi et al., 2015), adapted to our case where images contain multiple faces. Namely, we extract a VLAD descriptor for each image (computed using densely extracted SIFT descriptors (Lowe, 2004)) and cluster all images for each celebrity. This procedure results in per-celebrity clusters of near duplicate images. Dataset-wide clustering is obtained as the union of all per-celebrity clusters, where overlapping clusters (i.e. ones which share an image, which can happen because images contain multiple celebrities) are merged. Finally, de-duplication is performed by only keeping a single image from each cluster. Furthermore, images in common with the VGG Face Dataset (Parkhi et al., 2015) are removed as well.

Image annotation. Each face in each image is assigned to one of 2623 classes: 2622 celebrity names used to collect the dataset, or a special “unknown person” label if the person is not on the predefined celebrity list; the “unknown” people are used as distractors.

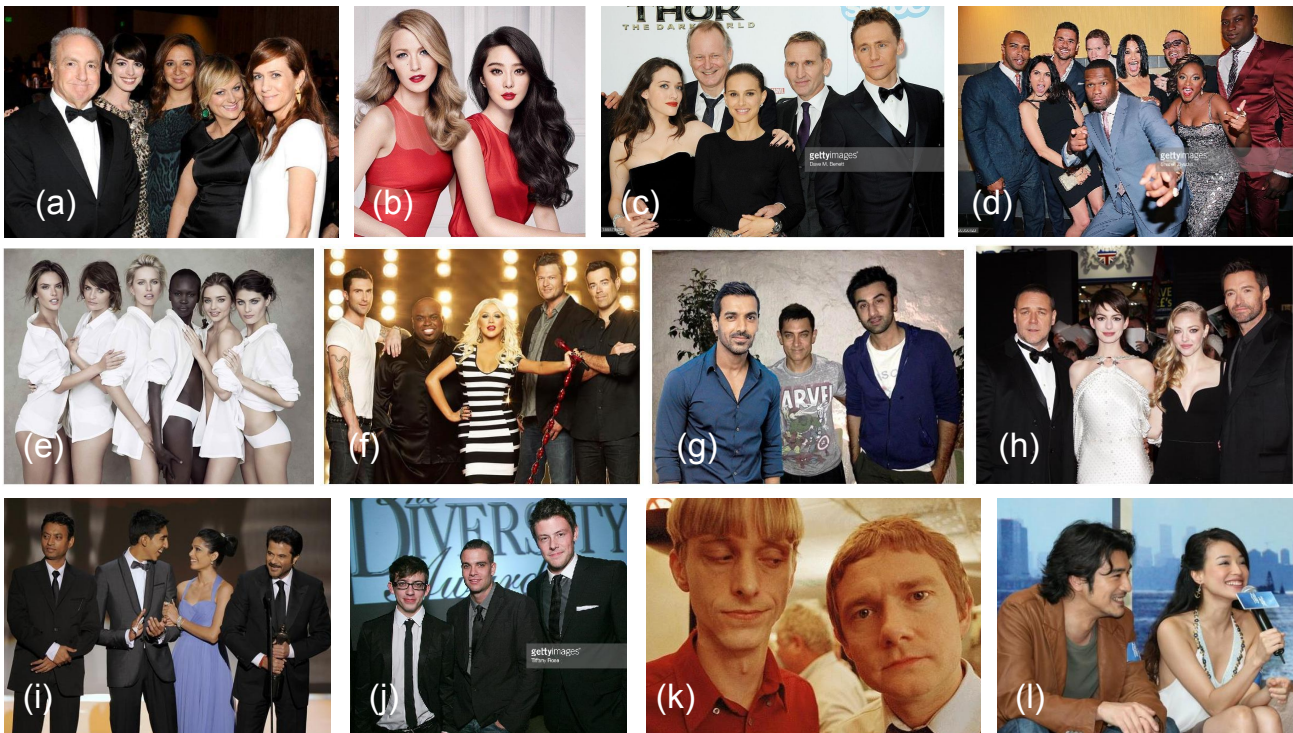


Fig. 4: **Example images of the *Celebrity Together* Dataset.** Note that only those celebrities who appear in the VGG Face Dataset are listed, as the rest are labelled as ‘unknown’. (a) Amy Poehler, Anne Hathaway, Kristen Wiig, Maya Rudolph. (b) Bingbing Fan, Blake Lively. (c) Kat Dennings, Natalie Portman, Tom Hiddleston. (d) Kathrine Narducci, Naturi Naughton, Omari Hardwick, Sinqua Walls. (e) Helena Christensen, Karolina Kurkova, Miranda Kerr. (f) Adam Levine, Blake Shelton, CeeLo Green. (g) Aamir Khan, John Abraham, Ranbir Kapoor. (h) Amanda Seyfried, Anne Hathaway, Hugh Jackman. (i) Anil Kapoor, Irrfan Khan. (j) Cory Monteith, Kevin McHale, Mark Salling. (k) Martin Freeman, Mackenzie Crook. (l) Takeshi Kaneshiro, Qi Shu. Additional examples of the dataset images are given in the supplementary material.

As the list of celebrities is the same as that used in the VGG Face Dataset (Parkhi et al., 2015), we use the pre-trained VGG-Face CNN (Parkhi et al., 2015) to aid with annotation by using it to predict the identities of the faces in the images. Combining the very confident CNN classifications with our prior belief of who is depicted in the image (i.e. the query terms), results in many good quality automatic annotations, which further decreases the manual annotation effort and costs. But choosing thresholds for deciding which images need annotation can be tricky, as we need to consider two cases: (i) if a face in an image belongs to one of the query names used for downloading that image, or (ii) if the face does not belong to the query names. The two cases require very different thresholds, as explained in the following.

Identities in the query text. We first consider the case where the predicted face (using VGG-Face) matches the corresponding query words for downloading that image. In this case, there is a very strong prior that the predicted face is correctly labelled as the predicted celebrity was explicitly searched for. Therefore, if the face is scored higher than 0.2 by the CNN, it is considered as being correctly labelled, otherwise

it is sent for human annotation. As another way of including low scoring predictions, if one of the query names is ranked within top 5 out of the 2622 celebrities by the CNN, the face is also sent for annotation. A face that does not pass any of the automatic or manual annotation requirements, is considered to be an “unknown” person.

Identities not in the query text. The next question is: if a face is predicted to be one of the 2622 celebrities with a high confidence (CNN score) but it does not match any query celebrities, can we automatically label it as a celebrity without human annotation? In this situation, the CNN is much less likely to be correct as the predicted celebrity was not explicitly searched for. Therefore, it has to pass a much stricter CNN score threshold of 0.8 in order to be considered to be correctly labelled without need for manual annotation. On the other hand, empirically we find that a prediction scored below 0.4 is always wrong, and is therefore automatically assigned the “unknown” label. The remaining case, a face with score between 0.4 and 0.8, should be manually annotated, but to save time and human effort we simply remove the image from the dataset.

Table 1: **Distribution of faces per image in the ‘Celebrity Together’ Dataset.**

| | | | | | |
|-------------------|------|-----|-----|----|-----|
| No. faces / image | 2 | 3 | 4 | 5 | >5 |
| No. images | 113k | 43k | 19k | 9k | 10k |

Table 2: **Distribution of annotations per image in the ‘Celebrity Together’ Dataset.**

| | | | | | | |
|-------------------|-----|-----|-----|----|------|------|
| No. celeb / image | 1 | 2 | 3 | 4 | 5 | >5 |
| No. images | 88k | 89k | 12k | 3k | 0.7k | 0.3k |

5 Experiments and results

In this section we investigate four aspects: first, in Sec. 5.1 we study the performance of different models (SetNet and baselines) as the number of faces per image in the dataset is increased. Second, we compare the performance of SetNet and the best baseline model on the real-world *Celebrity Together* dataset in Sec. 5.2. Third, the trade-off between time complexity and set retrieval quality is investigated in Sec. 5.3. Fourth, in Sec. 5.4, we demonstrate that SetNet learns to increase the descriptor orthogonality, which is good for aggregation.

Note, in all the experiments, there is no overlap between the query identities used for testing and the identities used for training the network, as the VGG Face Dataset (Parkhi et al., 2015) (used for testing, e.g. for forming the *Celebrity Together* dataset) and the VGGFace2 Dataset (Cao et al., 2018) (used for training) share no common identities.

Evaluation protocol. We use Normalized Discounted Cumulative Gain (Järvelin and Kekäläinen, 2002) (nDCG) to evaluate set retrieval performance, as it can measure how well images containing *all* the query identities and also *subsets* of the queries are retrieved. For this measurement, images have different relevance, not just a binary positive/negative label; the relevance of an image is equal to the number of query identities it contains. We report nDCG@10 and nDCG@30, where nDCG@N is the nDCG for the ranked list cropped at the top N retrievals. nDCG is computed as the ratio between DCG and the ideal DCG computed on the ground-truth ranking, where DCG is defined as:

$$DCG@N = \sum_{i=1}^N (2^{rel(i)} - 1) / \log_2(i + 1) \quad (3)$$

where $rel(i)$ denotes the relevance of the i th retrieved image. nDCGs are written as percentages, so the scores range between 0 and 100.

5.1 Stress test

In this test, we aim to investigate how different models perform with increasing number of faces per set (image) in the

test dataset. The effects of varying the number of faces per set used for training are also studied. One randomly sampled face example per query identity is used to query the dataset. The experiment is repeated 10 times using different face examples, and the nDCG scores are averaged.

Test dataset synthesis. A base dataset with 64k face sets of 2 faces each is synthesized, using only the face images of labelled identities in the *Celebrity Together* dataset. A random sample of 100 sets of 2 identities are used as queries, taking care that the two queried celebrities do appear together in some dataset face sets. To obtain four datasets of varying difficulty, 0, 1, 2 and 3 distractor faces per set are sampled from the unlabelled face images in *Celebrity Together* Dataset, taking care to include only true distractor people, i.e. people who are not in the list of labelled identities in the *Celebrity Together* dataset. Therefore, all four datasets contain the same number of face sets (64k) but have a different number of faces per set, ranging from 2 to 5. Importantly, by construction, the relevance of each set to each query is the same across all four datasets, which makes the performance numbers comparable across them.

Methods. The *SetNet* models are trained as described in Sec. 3.4, where the suffix ‘-2’ or ‘-3’ denotes whether 2- or 3-element sets are used during training. For SetNet, the optional suffix ‘+W’ means that the set descriptors are whitened. For example, *SetNet-2+W* is a model trained with 2-element sets and whitening. Whereas for baselines, ‘+W’ indicates whether the face descriptors have been whitened and L2-normalized before aggregation. We further investigate the effect of performing whitening after aggregation for the baselines, indicated as ‘+W (*W* after agg.)’. In this test, both SetNet and the baseline use ResNet-50 with 128-D feature output as the feature extractor network.

Baselines follow the same naming convention, where the architectural difference from the SetNet is that the aggregator block is replaced with average-pooling followed by L2-normalization, as shown in Fig. 2 (i.e. they use the same feature extractor network, data augmentation, optional whitening, etc.). The baselines are trained in the same manner as SetNet. The exceptions are *Baseline* and *Baseline+W*, which simply use the feature extractor network with average-pooling, but no training. It is important to note that training the modified ResNet-50 and SENet-50 networks on the VGGFace2 dataset (Cao et al., 2018) provides very strong baselines (referred to as *Baseline*). Although the objective of this paper is not face classification, to demonstrate the performance of this baseline network, we test it on the public IARPA Janus Benchmark A (IJB-A dataset) (Klare et al., 2015). Specifically, we follow the same test procedure for the 1:N Identification task described in (Cao et al., 2018). In terms of the true positive identification rate (TPIR), the ResNet-50 128-D network achieves 0.975, 0.993 and 0.994

for the top 1, 5 and 10 ranking respectively, which is on par with the state-of-the-art networks in (Cao et al., 2018).

For reference, an upper bound performance (*Descriptor-per-element*, see Sec. 5.3 for details) is also reported, where no aggregation is performed and all descriptors for all elements are stored.

Results. From the results in Fig. 5 it is clear that *SetNet-2+W* and *SetNet-3+W* outperform all baselines. As Fig. 6 shows, nDCG@30 generally follows a similar trend to nDCG@10: SetNet outperforms all the baselines by a large margin and, moreover, the gap increases as the number of elements per set increases. As expected, the performance of all models decreases as the number of elements per set increases due to larger cross-element interference. However, *SetNet+W* deteriorates more gracefully (the margin between it and the baselines increases), demonstrating that our training makes SetNet learn representations which minimise the interference between elements. The set training is beneficial for all architectures, including SetNet and baselines, as models with suffixes ‘-2’ and ‘-3’ (set training) achieve better results than those without (no set training).

Whitening improves the performance for all architectures when there are more than 2 elements per set, regardless whether the whitening is applied before or after the aggregation. This is a somewhat surprising result since adding whitening only happens after the network is trained. However, using whitening is common in the retrieval community as it is usually found to be very helpful (Arandjelović and Zisserman, 2013; Jégou and Chum, 2012), but has also been used recently to improve CNN representations (Radenović et al., 2016; Sun et al., 2017). Radenović et al. (2016) train a discriminative version of whitening for retrieval, while Sun et al. (2017) reduce feature correlations for pedestrian retrieval by formulating the SVD as a CNN layer. It is likely that whitening before aggregation is beneficial also because it makes descriptors more orthogonal to each other, which helps to reduce the amount of information lost by aggregation. However, *SetNet* gains much less from whitening, which may indicate that it learns to produce more orthogonal face descriptors. This claim is investigated further in Sec. 5.4.

It is also important to note that, as illustrated by Fig. 6b, the cardinality of the sets used for training does not affect the performance much, regardless of the architecture. Therefore, training with a set size of 2 or 3 is sufficient to learn good set representations which generalize to larger sets.

5.2 Evaluating on the Celebrity Together dataset

Here we evaluate the SetNet performance on the full *Celebrity Together* dataset.

Test dataset. The dataset is described in Sec. 4. To increase the retrieval difficulty, random 355k distractor images are

Table 3: **Number of images and faces in the test dataset.** The test dataset consists of the *Celebrity Together* dataset and distractor images from the MS-Celeb-1M dataset (Guo et al., 2016).

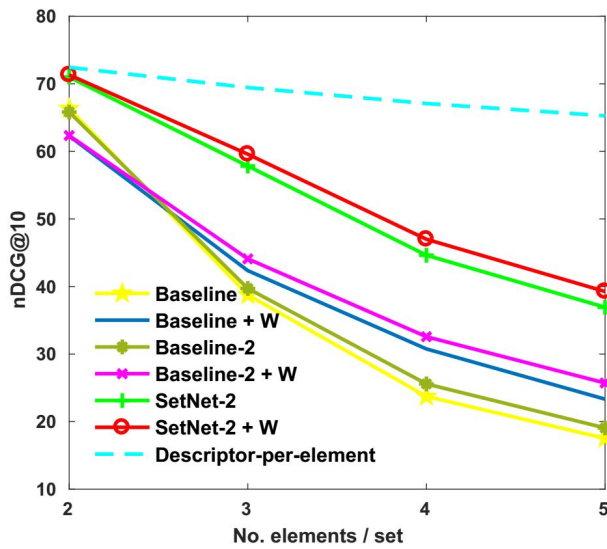
| | Celebrity Together | Distractors from MS1M | Total |
|--------|--------------------|-----------------------|-------|
| Images | 194k | 355k | 549k |
| Faces | 546k | 1M | 1546k |

sampled from the MS-Celeb-1M Dataset (Guo et al., 2016), as before taking care to include only true distractor people. The sampled distractor sets are constructed such that the number of faces per set follows the same distribution as in the *Celebrity Together* dataset. The statistics of the resultant test dataset are shown in Table 3. There are 1000 test queries, formed by randomly sampling 500 queries containing two celebrities and 500 queries containing three celebrities, under the restriction that the queried celebrities do appear together in some dataset images.

Experimental setup and baseline. In this test we consider two scenarios: first, where only one face example is available for each query identity, and second, where three face examples per query identity are available. In the second scenario, for each query identity, three face descriptors are extracted and aggregated to form a single enhanced descriptor which is then used to query the dataset.

In both scenarios the experiment is repeated 10 times using different face examples for each query identity, and the nDCG score is averaged. The best baseline from the stress test (Sec. 5.1) *Baseline-2+W* (modified ResNet with average-pooling), is used as the main comparison method. Moreover, we explore three additional variations of the baseline: (i) average-pooling the L2 normalized features before (rather than after) the final FC layer; (ii) (*Baseline-GM*), replacing the average-pooling with generalized mean pooling, $g(p) = \left(\frac{1}{n} \sum_{k=1}^n |x_k|^p\right)^{\frac{1}{p}}$, (Radenović et al., 2018) where the learnable parameter p is a scalar shared across all feature dimensions; and (iii) (*Baseline-GM* (p per dim.)), replacing the average-pooling with generalized mean pooling where the learnable parameter p is a vector with one value per dimension. Following (Radenović et al., 2018), the learnable parameter p is initialized to 3 for (ii) and to a vector of 3’s for (iii). All three variations are trained with 2 elements per set. The learnt p for (ii) is about 1.43. For (iii), the elements in the learnt p have various values mostly between 1.3 and 1.5. Note that for (ii) and (iii), whitening happens after the aggregation due to the restriction of the non-negative values in the descriptors.

Results. Table 4 shows that SetNets outperform the best baseline for all performance measures by a large margin, across different feature extractors (i.e. ResNet and SENet) and different feature dimensions (i.e. 128 and 256). The boost is

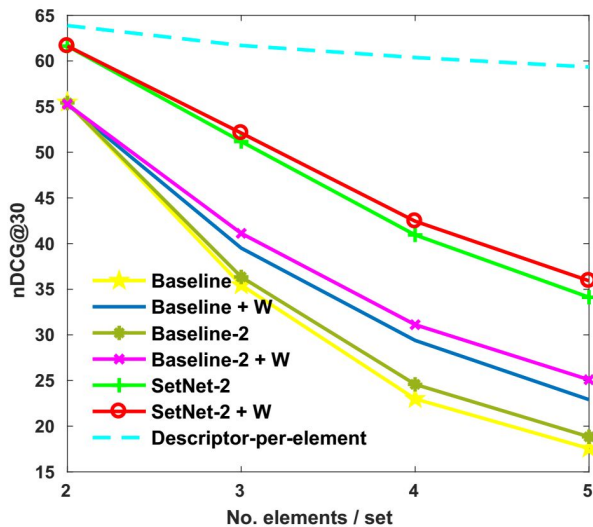


(a)

| Scoring model | 2/set | 3/set | 4/set | 5/set |
|-------------------------------|-------|-------|-------|-------|
| Baseline | 66.3 | 38.8 | 23.7 | 17.5 |
| Baseline-2 | 65.8 | 39.7 | 25.6 | 19.0 |
| Baseline-3 | 65.9 | 39.4 | 24.8 | 18.4 |
| SetNet | 71.1 | 55.1 | 43.2 | 34.9 |
| SetNet-2 | 71.0 | 57.7 | 44.6 | 36.9 |
| SetNet-3 | 71.9 | 57.9 | 44.7 | 37.0 |
| Baseline + W | 62.3 | 42.3 | 30.8 | 23.3 |
| Baseline-2 + W | 62.3 | 44.1 | 32.6 | 25.7 |
| Baseline-3 + W | 62.1 | 44.0 | 32.3 | 25.6 |
| Baseline-3 + W (W after agg.) | 62.2 | 44.0 | 32.2 | 25.6 |
| SetNet + W | 71.2 | 57.5 | 45.7 | 37.8 |
| SetNet-2 + W | 71.3 | 59.5 | 47.0 | 39.3 |
| SetNet-3 + W | 71.8 | 59.8 | 47.1 | 39.3 |
| Desc-per-element | 72.4 | 69.4 | 67.1 | 65.3 |

(b)

Fig. 5: **Stress test comparison of nDCG@10 of different models.** There are 100 query sets, each with two identities. (a) nDCG@10 for different number of elements (faces) per set (image) in the test dataset. (b) Table of nDCG@10 of stress test. Columns corresponds to the four different test datasets defined by the number of elements (faces) per set.



(a)

| Scoring model | 2/set | 3/set | 4/set | 5/set |
|-------------------------------|-------|-------|-------|-------|
| Baseline | 55.5 | 35.5 | 23.0 | 17.6 |
| Baseline-2 | 55.4 | 36.3 | 24.6 | 18.8 |
| Baseline-3 | 55.3 | 35.9 | 23.9 | 18.3 |
| SetNet | 61.1 | 49.2 | 39.1 | 32.2 |
| SetNet-2 | 61.6 | 51.1 | 40.9 | 34.1 |
| SetNet-3 | 61.5 | 51.2 | 41.0 | 34.2 |
| Baseline + W | 55.2 | 39.5 | 29.4 | 22.9 |
| Baseline-2 + W | 55.3 | 41.1 | 31.1 | 25.1 |
| Baseline-3 + W | 55.2 | 41.0 | 30.9 | 25.0 |
| Baseline-3 + W (W after agg.) | 55.2 | 41.0 | 30.9 | 25.0 |
| SetNet + W | 61.4 | 50.5 | 40.7 | 34.5 |
| SetNet-2 + W | 61.6 | 52.1 | 42.4 | 35.9 |
| SetNet-3 + W | 61.2 | 52.2 | 42.5 | 36.0 |
| Desc-per-element | 63.9 | 61.7 | 60.4 | 59.3 |

(b)

Fig. 6: **Stress test comparison of nDCG@30 of different models.** Columns corresponds to the four different test datasets defined by the number of elements (faces) per set.

particularly impressive when ResNet with 128-D output is used and only one face example is available for each query identity, where *Baseline-2+W* is beaten by 9.1% and 10.0% at nDCG@10 and nDCG@30 respectively. As we can see, performing the average-pooling before the FC layer in the feature extractor brings a marginal increase in the performance for the *Baseline-2+W*. A slightly larger enhancement is achieved by replacing the average-pooling in *Baseline-*

2+W by the generalized mean with a learnable parameter p . In practice, we find that using a shared value of p for all dimensions of the descriptors results in the best baseline model i.e. *Baseline-GM-2+W*. Although the baseline method is improved by a better (and learnable) mean computation method, the gap between the baseline models and SetNet is still significant.

Table 4: **Set retrieval performance on the test set.** D_e is the output feature dimension of the feature extractor CNN, and D is the dimension of the output feature dimension of SetNet. Q is the number of identities in the query. There are 500 queries with $Q = 2$, and 500 with $Q = 3$. N_{ex} is the number of available face examples for each identity. N_{qd} is the number of descriptors actually used for querying.

| Scoring model | Feature extractor | D_e | D | N_{qd} | Scenario 1: $N_{ex} = 1$ | | Scenario 2: $N_{ex} = 3$ | |
|-----------------------------------|-------------------|-------|-----|----------|--------------------------|-------------|--------------------------|-------------|
| | | | | | nDCG@10 | nDCG@30 | nDCG@10 | nDCG@30 |
| Baseline-2 + W | ResNet | 128 | - | Q | 50.0 | 49.4 | 56.6 | 56.0 |
| Baseline-2 + W (agg. before FC) | ResNet | 128 | - | Q | 50.2 | 49.5 | 56.6 | 56.0 |
| Baseline-GM-2 + W | ResNet | 128 | - | Q | 51.0 | 50.6 | 57.2 | 56.9 |
| Baseline-GM-2 + W (p per dim.) | ResNet | 128 | - | Q | 50.9 | 50.4 | 57.0 | 56.8 |
| SetNet-3 + W | ResNet | 128 | 128 | Q | 59.1 | 59.4 | 63.8 | 64.1 |
| SetNet-3 + W w/ query agg. | ResNet | 128 | 128 | 1 | 58.7 | 59.4 | 62.9 | 64.1 |
| Baseline-2 + W | SENet | 128 | - | Q | 52.9 | 52.5 | 59.6 | 59.5 |
| SetNet-3 + W | SENet | 128 | 128 | Q | 59.5 | 59.5 | 63.7 | 64.5 |
| SetNet-3 + W w/ query agg. | SENet | 128 | 128 | 1 | 59.1 | 59.5 | 63.4 | 64.0 |
| Baseline-2 + W | ResNet | 256 | - | Q | 56.8 | 57.8 | 62.5 | 64.2 |
| SetNet-3 + W | ResNet | 256 | 256 | Q | 61.2 | 62.6 | 66.0 | 68.9 |
| SetNet-3 + W w/ query agg. | ResNet | 256 | 256 | 1 | 60.3 | 62.4 | 65.1 | 68.8 |
| Baseline-2 + W | SENet | 256 | - | Q | 58.2 | 60.8 | 64.2 | 66.2 |
| SetNet-3 + W | SENet | 256 | 256 | Q | 62.6 | 64.8 | 67.3 | 70.1 |
| SetNet-3 + W w/ query agg. | SENet | 256 | 256 | 1 | 61.9 | 64.5 | 66.3 | 69.6 |

Similar improvement appears for SENet-based SetNet: 6.6% at nDCG@10 and 7% at nDCG@30. When a feature dimension of 256 is used, we also observe that *SetNet-3+W* outperforms *Baseline-2+W* by a significant amount, e.g. 4.4% at nDCG@10 on both ResNet and SENet. Note that the gap between the baseline and SetNet is smaller when we use 256-D set-level descriptors rather than 128-D. This indicates that the superiority of SetNet is more obvious with lower dimensionality. The improvement is also significant for the second scenario where three face examples are available for each query identity. For example, an improvement of 7.2% and 8.1% over the baseline is observed on ResNet with 128-D output, and 4.1% and 5% on SENet. We can also conclude that SENet achieves better results than ResNet as it produces better face descriptors. In general, the results demonstrate that our trained aggregation method is indeed beneficial since it is designed and trained end-to-end exactly for the task in hand. Fig. 1 shows the top 3 retrieved images out of 549k images for two examples queries using SetNet (images are cropped for better viewing).

Query aggregation. We also investigate a more efficient method to query the database for multiple identities. Namely, we aggregate the descriptors of all the query identities using SetNet to produce a single descriptor which represents all query identities, and query with this single descriptor. In other words, we treat all the query images as a set, and then obtain a set-level query descriptor using SetNet. In the second scenario, when three face examples are available for each query identity, all of the descriptors are simply fed to SetNet to compute a single descriptor. With this query representation we obtain a slightly lower nDCG@10 compared to the original method shown in Table 4 (62.9 vs 63.8), and the same nDCG@30 (64.1). However, as will be seen in the

next section, this drop can be nullified by re-ranking, making *query aggregation* an attractive method due to its efficiency. In the second scenario, apart from aggregating the query face descriptors, we also investigated other ways of making use of multiple face examples per query, including scoring the dataset images with each face example separately followed by merging the scores for each image under some combination rules (e.g. mean, max, etc.). However, it turns out that simply aggregating the face descriptors for each query identity achieves the best performance and, moreover, it is the most efficient method as it adds almost no computational cost to the single-face-example scenario.

5.3 Efficient set retrieval

Our SetNet approach stores a single descriptor-per-set making it very fast though with potentially sacrificed accuracy. This section introduces some alternatives and evaluates trade-offs between set retrieval quality and retrieval speed. To evaluate computational efficiency formally with the big-O notation, let Q , F and N be the number of query identities, average number of faces per dataset image, and the number of dataset images, respectively, and let the face descriptor be D -dimensional. Recall that our SetNet produces a compact set representation which is also D -dimensional, and $D = 128$ or 256.

Descriptor-per-set (SetNet). Storing a single descriptor per set is very computationally efficient as ranking only requires computing a scalar product between Q query D -dimensional descriptors and each of the N dataset descriptors, passing them through a logistic function, followed by scoring the images by the sum of similarity scores, making this step

$O(NQD)$. For the more efficient *query aggregation* where only one query descriptor is used to represent all the query identities, this step is even faster with $O(ND)$. Sorting the scores is $O(N \log N)$. Total memory requirements are $O(ND)$.

Descriptor-per-element. Set retrieval can also be performed by storing all element descriptors, requiring $O(NFD)$ memory. Assuming there is no need for handling strange (e.g. Photoshopped) images, each query identity can be portrayed at most once in an image, and each face can only correspond to a single query identity. An image can be scored by obtaining all $Q \times F$ pairs of (query-identity, image-face) scores and finding the optimal assignment by considering it as a maximal weighted matching problem in a bipartite graph. Instead of solving the problem using the Hungarian algorithm which has computational complexity that is cubic in the number of faces and is thus prohibitively slow, we use a greedy matching approach. Namely, all (query-identity, image-face) matches are considered in decreasing order of similarity and added to the list of accepted matches if neither of the query person nor the image face have been added already. The complexity of this greedy approach is $O(QF \log(QF))$ per image. Therefore, the total computational complexity is $O(NQFD + NQF \log(QF) + N \log N)$. For our problem, we do not find any loss in retrieval performance compared to optimal matching, while being $7 \times$ faster.

Combinations by re-ranking. Borrowing ideas again from image retrieval (Philbin et al., 2007; Sivic and Zisserman, 2003), it is possible to combine the speed benefits of the faster methods with the accuracy of the slow descriptor-per-element method by using the former for initial ranking, and the latter to re-rank the top N_r results. The computational complexity is then equal to that of the fast method of choice, plus $O(N_r QFD + N_r QF \log(QF) + N_r \log N_r)$.

Pre-tagging. A fast but naive approach to set retrieval is to pre-tag all the dataset images offline with a closed-world of known identities by deeming a person to appear in the image if the score is larger than a threshold. Set retrieval is then performed by ranking images based on the intersection between the query and image tags. Pre-tagging seems straightforward, however, it suffers from two large limitations; first, it is very constrained as it only supports querying for a fixed set of identities which has to be predetermined at the offline tagging stage. Second, it relies on making hard decisions when assigning an identity to a face, which is expected to perform badly, especially in terms of recall. Note to obtain high precision (i.e. correct) results for tagging, 10 face examples are used for making the decision on whether each predetermined identity is in the database images. Thus tagging is a somewhat unfair baseline as all the other methods operate in a more realistic scenario of only having one to three examples available. The computational complexity is $O(NQ + N \log N)$

but pre-tagging is very fast in practice as querying can be implemented efficiently using an inverted index.

Experimental setup. The performance is evaluated on the 1000 test queries and on the same full dataset with distractors as in Sec. 5.2. N_r is varied in this experiment to demonstrate the trade-off between accuracy and retrieval speed. Here, there is one available face example for each identity, $N_{ex} = 1$. For the descriptor-per-element and pre-tagging methods, we use the Baseline + W features.

Speed test implementation. The retrieval speed is measured as the mean over all 1000 test query sets. The test is implemented in Matlab, and the measurements are carried out on a Xeon E5-2667 v2/3.30GHz, with only a single thread.

5.3.1 Results

Table 5 shows set retrieval results for the various methods together with the time it takes to execute a set query. The full descriptor-per-element approach is the most accurate one, but also prohibitively slow for most uses, taking more than 6 seconds to execute a query using 128-D descriptors (and 8 seconds for 256-D.) The descriptor-per-set (i.e. SetNet) approach with query aggregation is blazingly fast with only 0.01s per query using one descriptor to represent all query identities, but sacrifices retrieval quality to achieve this speed. However, taking the 128-D descriptor as an example, using SetNet for initial ranking followed by re-ranking achieves good results without a significant speed hit – the accuracy almost reaches that of the full slow descriptor-per-element (e.g. the gap is 0.3% for ResNet and 0.8% for SENet at nDCG@30), while being more than $35 \times$ faster. A even larger speed gain is observed using 256-D descriptor, namely about $45 \times$ faster than the desc-per-element method. Furthermore, by combining *desc-per-set* and *desc-per-element* it is possible to choose the trade-off between speed and retrieval quality, as appropriate for specific use cases. For a task where speed is crucial, *desc-per-set* can be used with few re-ranking images (e.g. 100) to obtain a $212 \times$ speedup over the most accurate method (*desc-per-element*). For an accuracy-critical task, it is possible to re-rank more images while maintaining a reasonable speed.

Baselines. The best baseline method *Baseline-GM-2+W* is inferior to our proposed SetNet even when combined with re-ranking. This is mainly because the initial ranking using *Baseline-GM-2+W* does not have a large enough recall – it does not retrieve a sufficient number of target images in the top 2000 ranks, so re-ranking is not able to reach the SetNet performance.

Pre-tagging. Pre-tagging achieves better results than *desc-per-set* using SetNet descriptors without re-ranking. This is reasonable as pre-tagging should be categorized into the desc-per-element method, i.e. it performs offline face recognition

Table 5: **Retrieval speed vs quality trade-off with varied number of re-ranking images.** Retrieval performance, average time required to execute a set query and speedup over *Desc-per-element* are shown for each method. ‘Re.’ denotes re-ranking, D denotes the dimension of both the set-level descriptors and the descriptors used in pre-tagging method, and N_r denotes the number of re-ranked images. The evaluation is on the 1000 test queries and on the same full dataset with distractors as in Sec. 5.2. [†] Note that *Pre-tagging* is an unfair baseline, as explained in Sec. 5.3.

| Scoring method | Architecture | Feature extractor | D | N_r | Without query aggregation | | | | With query aggregation | | | |
|------------------------|--------------------------|-------------------|-----|-------|---------------------------|----------|--------|---------|------------------------|----------|--------|---------|
| | | | | | nDCG @10 | nDCG @30 | Timing | Speedup | nDCG @10 | nDCG @30 | Timing | Speedup |
| Desc-per-set | Baseline-GM-2 + W | ResNet | 128 | - | 51.0 | 50.6 | 0.11s | 57.5× | 50.6 | 50.6 | 0.01s | 635× |
| Desc-per-set + Re. | Baseline-GM-2 + W | ResNet | 128 | 2000 | 78.5 | 76.2 | 0.28s | 22.7× | 78.5 | 76.2 | 0.03s | 212× |
| Desc-per-element | Pre-tagging [†] | ResNet | 128 | - | 65.7 | 68.6 | 0.01s | 635× | - | - | - | - |
| Desc-per-element + Re. | Pre-tagging [†] | ResNet | 128 | 2000 | 84.6 | 82.4 | 0.18s | 35.3× | - | - | - | - |
| Desc-per-set | SetNet-3 + W | ResNet | 128 | - | 59.1 | 59.4 | 0.11s | 57.5× | 58.7 | 59.4 | 0.01s | 635× |
| Desc-per-set + Re. | SetNet-3 + W | ResNet | 128 | 100 | 76.5 | 70.1 | 0.13s | 48.8× | 76.4 | 70.1 | 0.03s | 212× |
| Desc-per-set + Re. | SetNet-3 + W | ResNet | 128 | 1000 | 84.2 | 80.0 | 0.20s | 31.8× | 84.1 | 80.0 | 0.10s | 63.5× |
| Desc-per-set + Re. | SetNet-3 + W | ResNet | 128 | 2000 | 85.3 | 81.4 | 0.28s | 22.7× | 85.3 | 81.4 | 0.18s | 35.3× |
| Desc-per-element | Baseline + W | ResNet | 128 | - | 85.4 | 81.7 | 6.35s | - | - | - | - | - |
| Desc-per-set + Re. | SetNet-3 + W | SENet | 128 | 2000 | 85.8 | 81.0 | 0.28s | 22.7× | 85.8 | 81.0 | 0.18s | 35.3× |
| Desc-per-element | Baseline + W | SENet | 128 | - | 85.8 | 81.8 | 6.35s | - | - | - | - | - |
| Desc-per-set + Re. | SetNet-3 + W | ResNet | 256 | 2000 | 85.2 | 82.1 | 0.40s | 21.3× | 85.2 | 82.1 | 0.19s | 44.9× |
| Desc-per-element | Baseline + W | ResNet | 256 | - | 85.6 | 82.3 | 8.53s | - | - | - | - | - |
| Desc-per-set + Re. | SetNet-3 + W | SENet | 256 | 2000 | 85.7 | 83.4 | 0.40s | 21.3× | 85.7 | 83.4 | 0.19s | 44.9× |
| Desc-per-element | Baseline + W | SENet | 256 | - | 85.9 | 83.5 | 8.53s | - | - | - | - | - |

on individual face descriptors. However, it is significantly lower than SetNet even with only 100 re-ranking images, e.g. 65.7% vs. 76.5% in nDCG@10. Lastly, for a more fair comparison, we perform re-ranking for the pre-tagging baseline. With the same number of re-ranked images (i.e. 2000), desc-per-set + re-ranking beats pre-tagging in nDCG@10 (85.3% vs. 84.6%) while having slightly lower nDCG@30. Note that the pre-tagging method makes use of 10 face examples per identity for face recognition, whereas only one face example is available for each query identity for SetNet. Most importantly, the pre-tagging method suffers from the limitation of retrieving only a closed-world set of identities. In contrast, desc-per-set + re-ranking, is open-world as the query faces can simply be supplied at run-time. Thus it is strongly preferred over pre-tagging in practice.

Retrieval examples. We visualize the performance of the set retrieval system based on descriptors produced by SetNet by showing some retrieval examples. The top ranked 5 images (ordered column-wise) for several queries are shown in Fig. 7, 8, 9 (images are cropped for displaying purposes in order to see the faces better). Notably, the nDCG@5 (the quality of the top 5 retrievals) is equal to 1 for all examples, meaning that images are correctly ranked according to the size of their overlap with the query set. The retrieval is performed by desc-per-set + re-ranking using descriptors produced by a 128-D ResNet-based SetNet.

5.4 Descriptor orthogonality

As observed in Sec. 5.1, whitening face descriptors before aggregation improves the performance of baselines. This section investigates this phenomenon further as well as the behaviour of face descriptors learnt by SetNet.

We hypothesize that whitening helps because it decorrelates each dimension of the descriptors, and consequently descriptors will interfere less when added to each other. Furthermore, we expect SetNet to automatically learn such behaviour in order to minimize the interference between descriptors after aggregation. To verify this, we measure the extent to which face descriptors are orthogonal to each other as follows. We compute the Gram matrix of face descriptors for 2622 identities in the VGG Face Dataset and measure the deviation G_{diff} between the computed Gram matrix and an identity matrix (the Gram matrix of fully orthogonal descriptors):

$$G_{diff} = \|G - I\|_{Frob} \quad (4)$$

where G is the Gram matrix and I is the identity matrix. Smaller G_{diff} corresponds to more orthogonal descriptors.

Implementation details. G_{diff} is computed in four steps: first, 100 faces are randomly sampled for each identity in the VGG Face Dataset, and a feature vector for each face sample is extracted by the network; second, a single identity descriptor is obtained for each identity by averaging the 100 face descriptors followed by L2-normalization; third, the 2622×2622 Gram matrix is computed by taking the scalar product between all possible pairs of identity descriptors

Table 6: **Difference between Gram matrix and identity matrix** G_{diff} . The Gram matrix is computed over 2622 identities in VGG Face Dataset. D denotes the dimension of the set-level descriptors.

| Model | Feature extractor | D | Not whitened | Whitened |
|------------|-------------------|-----|--------------|----------|
| Baseline-2 | ResNet-50 | 128 | 399 | 276 |
| SetNet-3 | ResNet-50 | 128 | 274 | 268 |

after mean subtraction and re-normalization. We compute G_{diff} using non-whitened and whitened features of the best baseline network, *Baseline-2*, and SetNet. Both networks are trained on the VGGFace2 dataset (Cao et al., 2018), and their corresponding whitening transformations are computed on the same dataset. To evaluate descriptor orthogonality, the Gram matrix and G_{diff} are computed using the independent set of identities of VGGFace (Parkhi et al., 2015).

Results. As Table 6 shows, face features produced by *SetNet-3* are much more orthogonal than the ones from *Baseline-2*, confirming our intuition that this behaviour should naturally emerge from our training procedure. Whitening reduces G_{diff} for both *Baseline-2* and *SetNet-3*, as expected, but the reduction is small for *SetNet-3* as its descriptors are already quite orthogonal, while it is large for *Baseline-2* since those are not. Furthermore, SetNet without whitening has a smaller G_{diff} than even the whitened baseline, demonstrating that SetNet learns to produce descriptors which are well suited for aggregation.

6 Conclusion

We have considered a new problem of set retrieval, discussed multiple different approaches to tackle it, and evaluated them on a specific case of searching for sets of faces. Our learnt compact set representation, produced using the SetNet architecture and trained in a novel manner directly for the set retrieval task, beats all baselines convincingly. Furthermore, due to its high speed it can be used for fast set retrieval in large image datasets. The set retrieval problem has applications beyond multiple faces in an image. For example, a similar situation would also apply for the task of video retrieval when the elements themselves are images (frames), and the set is a video clip or shot.

We have also introduced a new dataset, *Celebrity Together*, which can be used to evaluate set retrieval performance and to facilitate research on this new topic. The dataset is available at http://www.robots.ox.ac.uk/~vgg/data/celebrity_together/.

Acknowledgements This work was funded by an EPSRC studentship and EPSRC Programme Grant Seebibyte EP/M013774/1.

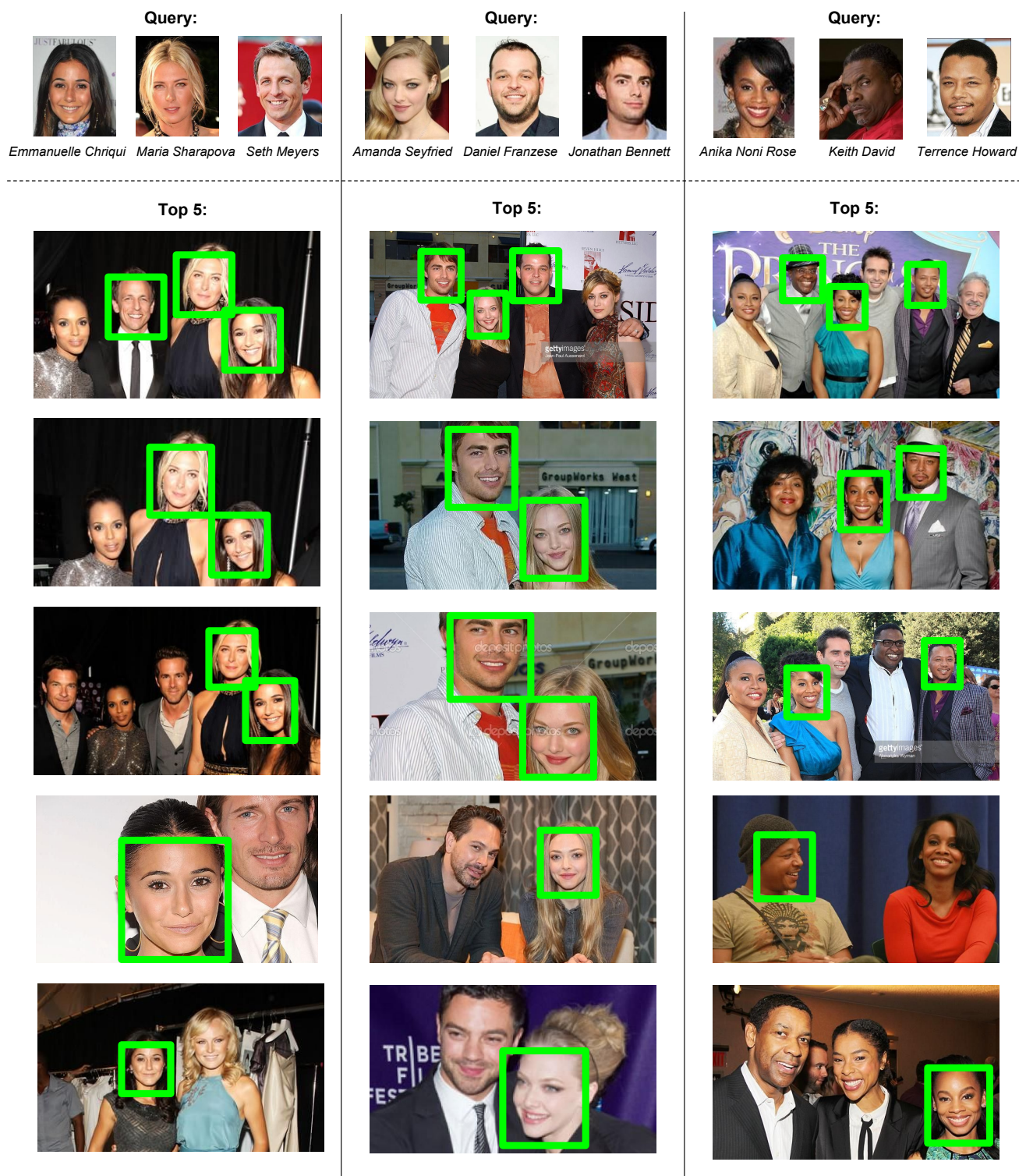


Fig. 7: **Top 5** ranked images returned by the SetNet based descriptor-per-set retrieval. The query identities are highlighted by green bounding boxes.

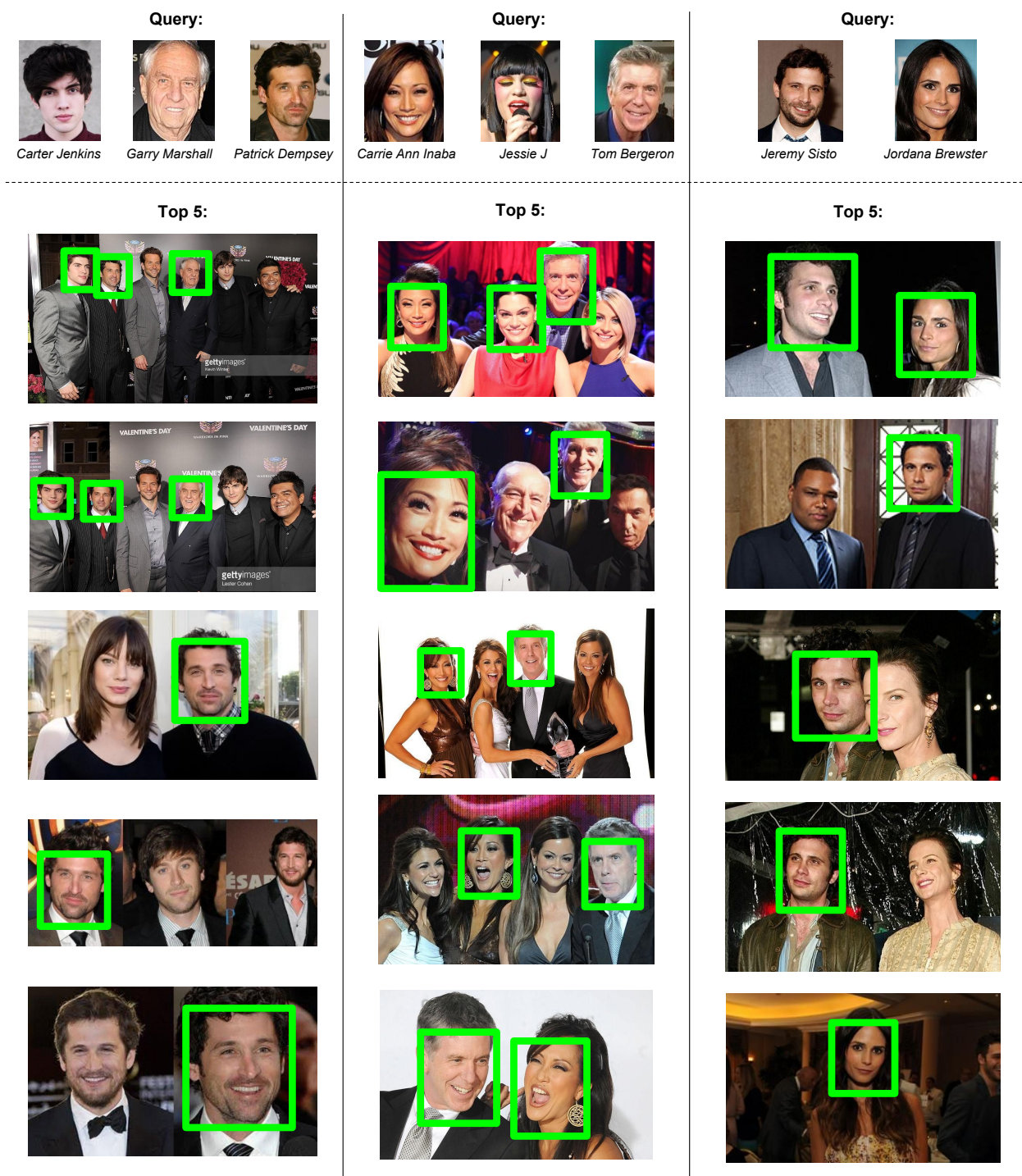


Fig. 8: Top 5 ranked images returned by the SetNet based descriptor-per-set retrieval. The query identities are highlighted by green bounding boxes.

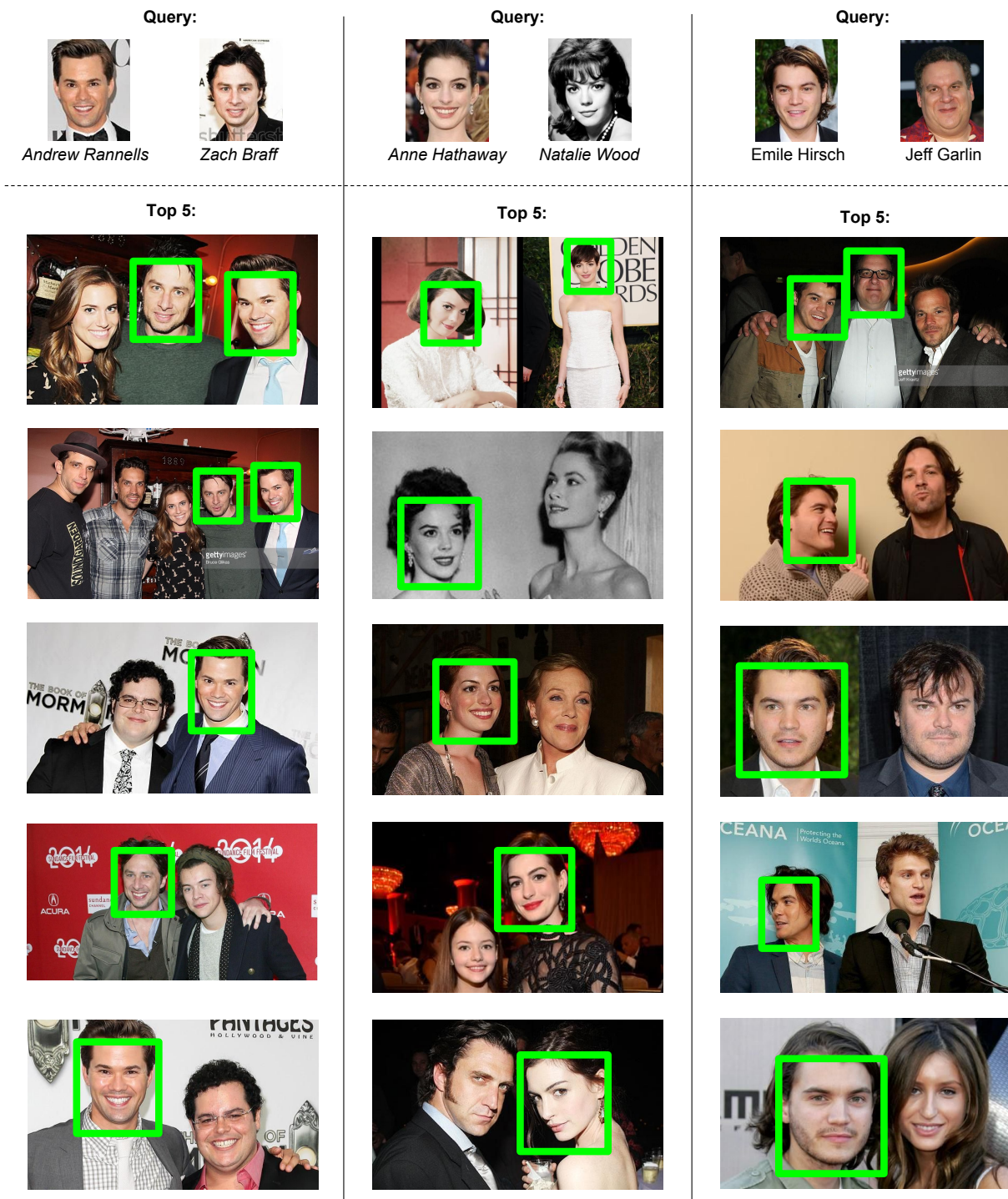


Fig. 9: Top 5 ranked images returned by the SetNet based descriptor-per-set retrieval. The query identities are highlighted by green bounding boxes.

References

- Arandjelović R, Zisserman A (2013) All about VLAD. In: Proc. CVPR
- Arandjelović R, Gronat P, Torii A, Pajdla T, Sivic J (2016) NetVLAD: CNN architecture for weakly supervised place recognition. In: Proc. CVPR
- Cao Q, Shen L, Xie W, Parkhi OM, Zisserman A (2018) VGGFace2: A dataset for recognising faces across pose and age. In: Proc. Int. Conf. Autom. Face and Gesture Recog.
- Chatfield K, Lempitsky V, Vedaldi A, Zisserman A (2011) The devil is in the details: an evaluation of recent feature encoding methods. In: Proc. BMVC.
- Chatfield K, Simonyan K, Zisserman A (2014) Efficient on-the-fly category retrieval using convnets and gpus. In: Proc. ACCV
- Chatfield K, Arandjelović R, Parkhi OM, Zisserman A (2015) On-the-fly learning for visual search of large-scale image and video datasets. *International Journal of Multimedia Information Retrieval*
- Chum O, Philbin J, Sivic J, Isard M, Zisserman A (2007) Total recall: Automatic query expansion with a generative feature model for object retrieval. In: Proc. ICCV
- Delhumeau J, Gosselin PH, Jégou H, Pérez P (2013) Revisiting the VLAD image representation. In: Proc. ACMM
- Donahue J, Jia Y, Vinyals O, Hoffman J, Zhang N, Tzeng E, Darrell T (2013) Decaf: A deep convolutional activation feature for generic visual recognition. CoRR abs/1310.1531
- Feng J, Karaman S, Chang S (2017) Deep image set hashing. In: 2017 IEEE Winter Conference on Applications of Computer Vision (WACV), IEEE, pp 1241–1250
- Guo Y, Zhang L, Hu Y, He X, Gao J (2016) MS-Celeb-1M: A dataset and benchmark for large-scale face recognition. In: Proc. ECCV
- Hamid Rezafofighi S, Kumar B, Milan A, Abbasnejad E, Dick A, Reid I (2017) DeepSetNet: Predicting sets with deep neural networks. In: Proc. CVPR
- He K, Zhang X, Ren S, Sun J (2016) Deep residual learning for image recognition. In: Proc. CVPR
- Hu J, Shen L, Sun G (2018) Squeeze-and-excitation networks. In: Proc. CVPR
- Ilse M, Tomczak J, Welling M (2018) Attention-based deep multiple instance learning. arXiv preprint arXiv:180204712
- Ioffe S, Szegedy C (2015) Batch normalization: Accelerating deep network training by reducing internal covariate shift. In: Proc. ICML
- Iscen A, Furon T, Gripon V, Rabbat M, Jégou H (2017) Memory vectors for similarity search in high-dimensional spaces. *IEEE Transactions on Big Data*
- Järvelin K, Kekäläinen J (2002) Cumulated gain-based evaluation of ir techniques. *ACM Transactions on Information Systems (TOIS)* 20(4):422–446
- Jégou H, Chum O (2012) Negative evidences and co-occurrences in image retrieval: the benefit of PCA and whitening. In: Proc. ECCV
- Jégou H, Zisserman A (2014) Triangulation embedding and democratic aggregation for image search. In: Proc. CVPR
- Jégou H, Douze M, Schmid C, Pérez P (2010) Aggregating local descriptors into a compact image representation. In: Proc. CVPR
- Jégou H, Perronnin F, Douze M, Sánchez J, Pérez P, Schmid C (2011) Aggregating local image descriptors into compact codes. *IEEE PAMI*
- Klare B, Klein B, Taborsky E, Blanton A, Cheney J, Allen K, Grother P, Mah A, Jain A (2015) Pushing the frontiers of unconstrained face detection and recognition: Iarpa janus benchmark a. In: Proc. CVPR, pp 1931–1939
- Kondor R, Jebara T (2003) A kernel between sets of vectors. In: Proc. ICML, AAAI Press
- Krizhevsky A, Sutskever I, Hinton GE (2012) ImageNet classification with deep convolutional neural networks. In: NIPS, pp 1106–1114
- Lee J, Lee Y, Kim J, Kosiorek A, Choi S, Teh YW (2018) Set transformer. arXiv preprint arXiv:181000825
- Li B, Xiao R, Li Z, Cai R, Lu BL, Zhang L (2011) Rank-SIFT: Learning to rank repeatable local interest points. In: Proc. CVPR, pp 1737–1744
- Li Y, Wang R, Liu H, Jiang H, Shan S, Chen X (2015) Two birds, one stone: Jointly learning binary code for large-scale face image retrieval and attributes prediction. In: Proc. ICCV, pp 3819–3827
- Liu Y, Yan J, Ouyang W (2017) Quality aware network for set to set recognition. In: Proc. CVPR, pp 5790–5799
- Lowe D (2004) Distinctive image features from scale-invariant keypoints. *IJCV* 60(2):91–110
- Nister D, Stewenius H (2006) Scalable recognition with a vocabulary tree. In: Proc. CVPR, pp 2161–2168
- Parkhi OM, Vedaldi A, Zisserman A (2015) Deep face recognition. In: Proc. BMVC.
- Perronnin F, Liu Y, Sánchez J, Poirier H (2010a) Large-scale image retrieval with compressed fisher vectors. In: Proc. CVPR
- Perronnin F, Sánchez J, Mensink T (2010b) Improving the Fisher kernel for large-scale image classification. In: Proc. ECCV
- Philbin J, Chum O, Isard M, Sivic J, Zisserman A (2007) Object retrieval with large vocabularies and fast spatial matching. In: Proc. CVPR
- Radenović F, Toliás G, Chum O (2016) CNN image retrieval learns from BoW: Unsupervised fine-tuning with hard examples. In: Proc. ECCV

- Radenović F, Tolias G, Chum O (2018) Fine-tuning cnn image retrieval with no human annotation. *IEEE PAMI*
- Razavian A, Azizpour H, Sullivan J, Carlsson S (2014) CNN Features off-the-shelf: an Astounding Baseline for Recognition. *CoRR abs/1403.6382*
- Santoro A, Raposo D, Barrett D, Malinowski M, Pascanu R, Battaglia P, Lillicrap T (2017) A simple neural network module for relational reasoning. In: *NIPS*, pp 4967–4976
- Schroff F, Kalenichenko D, Philbin J (2015) FaceNet: A unified embedding for face recognition and clustering. In: *Proc. CVPR*
- Sermanet P, Eigen D, Zhang X, Mathieu M, Fergus R, LeCun Y (2013) OverFeat: Integrated recognition, localization and detection using convolutional networks. *arXiv preprint arXiv:1312.6229*
- Shi B, Bai S, Zhou Z, Bai X (2015) Deeppano: Deep panoramic representation for 3-d shape recognition. *IEEE Signal Processing Letters* 22(12):2339–2343
- Siddiquie B, Feris R, Davis L (2011) Image ranking and retrieval based on multi-attribute queries. In: *Proc. CVPR, IEEE*, pp 801–808
- Sivic J, Zisserman A (2003) Video Google: A text retrieval approach to object matching in videos. In: *Proc. ICCV*, vol 2, pp 1470–1477
- Su H, Maji S, Kalogerakis E, Learned-Miller E (2015) Multi-view convolutional neural networks for 3d shape recognition. In: *Proc. ICCV*, pp 945–953
- Sun Y, Zheng L, Deng W, Wang S (2017) SVDNet for pedestrian retrieval. In: *Proc. ICCV*
- Taigman Y, Yang M, Ranzato M, Wolf L (2014) Deep-Face: Closing the gap to human-level performance in face verification. In: *IEEE CVPR*
- Torresani L, Szummer M, Fitzgibbon A (2010) Efficient object category recognition using classemes. In: *Proc. ECCV*, pp 776–789
- Vedaldi A, Lenc K (2015) Matconvnet: Convolutional neural networks for matlab. In: *Proc. ACMM*
- Vinyals O, Bengio S, Kudlur M (2016) Order matters: Sequence to sequence for sets. *Proc ICLR*
- Wang J, Yang J, Yu K, Lv F, Huang T, Gong Y (2010) Locality-constrained linear coding for image classification. In: *Proc. CVPR*
- Wang W, Wang R, Shan S, Chen X (2017) Discriminative covariance oriented representation learning for face recognition with image sets. In: *Proc. CVPR*, pp 5599–5608
- Yang B, Wang S, Markham A, Trigoni N (2018) Attentional aggregation of deep feature sets for multi-view 3d reconstruction. *arXiv preprint arXiv:1808.00758*
- Yang J, Ren P, Zhang D, Chen D, Wen F, Li H, Hua G (2017) Neural aggregation network for video face recognition. In: *Proc. CVPR*, pp 4362–4371
- Zaheer M, Kottur S, Ravanbakhsh S, Póczos B, Salakhutdinov R, Smola A (2017) Deep sets. In: *NIPS*, pp 3391–3401
- Zhang K, Zhang Z, Li Z, Qiao Y (2016) Joint face detection and alignment using multitask cascaded convolutional networks. *IEEE Signal Processing Letters* 23(10):1499–1503
- Zhong Y, Arandjelović R, Zisserman A (2016) Faces in places: Compound query retrieval. In: *Proc. BMVC*
- Zhou X, Yu K, Zhang T, Huang TS (2010) Image classification using super-vector coding of local image descriptors. In: *Proc. ECCV*